



## Journal of Advanced Research in Applied Mechanics

Journal homepage:  
[https://semarakilmu.com.my/journals/index.php/appl\\_mech/index](https://semarakilmu.com.my/journals/index.php/appl_mech/index)  
ISSN: 2289-7895



# Rice Husk for Adsorbing Dyes in Wastewater: Literature Review of Agricultural Waste Adsorbent, Preparation of Rice Husk Particles, Particle Size on Adsorption Characteristics with Mechanism and Adsorption Isotherm

Asep Bayu Dani Nandiyanto<sup>1,\*</sup>, Willy Cahya Nugraha<sup>2</sup>, Intan Yustia<sup>1</sup>, Risti Ragadhita<sup>1</sup>, Meli Fiandini<sup>1</sup>, Muksin Saleh<sup>3</sup>, Diana Rahayu Ningwulan<sup>2</sup>

<sup>1</sup> Departemen Kimia, Universitas Pendidikan Indonesia, Jl. Dr. Setiabudi 229, Bandung 40154, Indonesia

<sup>2</sup> Research Center for Environmental and Clean Technology, National Research and Innovation Agency, Jalan Cisitua Sangkuriang, 40135, Bandung, Indonesia

<sup>3</sup> Research Center for Process and Manufacturing Industry Technology, National Research and Innovation Agency, Kawasan Puspiptek Serpong 15314, Tangerang, Indonesia

### ARTICLE INFO

### ABSTRACT

#### Article history:

Received 28 January 2023

Received in revised form 10 April 2023

Accepted 15 April 2023

Available online 2 May 2023

#### Keywords:

Adsorption; dye; isotherms; rice husk; Sustainable Development Goals; turmeric

This study aims to evaluate the adsorption characteristics of unmodified natural rice husk particles (sizes of 74, 177, and 500  $\mu\text{m}$ ) in adsorbing dyes in wastewater. The adsorption isotherm analysis was performed in batch mode. Turmeric was selected as a model for organic dyes. Ten isotherm models were used to predict and determine the characteristic parameters: Langmuir, Freundlich, Temkin, Dubinin-Radushkevich, Flory-Huggins, Fowler-Guggenheim, Hill-de-Boer, Jovanovic, Harkin Jura, and Halsey isotherm models. The adsorption isotherm analysis showed the phenomena that occur during adsorption are physical, with multilayer formation on the surface of the adsorbent and the occurrence of adsorbate-adsorbate repulsive interaction. The pore-filling molecules occur at the largest and medium particle sizes, whereas the small particle size has no pore-filling molecules. This study reveals that the natural rice husk (unmodified) could be employed as a low-cost and effective sorbent for wastewater treatment, supporting current issues in the Sustainable Development Goals (SDGs).

## 1. Introduction

The use of rice husk as an adsorbent has become increasingly popular, specifically, in agricultural countries, such as Indonesia [1]. Rice husk (20-22wt% of rice) is obtained during the rice milling process [2]. Rice husk has a high concentration of silica (about 96.34%). The prominent organic compounds found in rice husks are cellulose, hemicellulose, and lignin [3]. Rice husks are abundant and inexpensive, making the use of them in small industries challenging. The prospective use of rice husks opens ideas for supporting current issues in the sustainable development goals (SDGs).

\* Corresponding author.

E-mail address: [nandiyanto@upi.edu](mailto:nandiyanto@upi.edu)

<https://doi.org/10.37934/aram.106.1.113>

Rice husk is one of the abundant agricultural wastes. Many reports have been published regarding rice husk [4-8]. Although there have been many successful studies on the use of agricultural wastes as adsorbents (Table 1), previous studies have focused only on the synthesis and modification of the materials and their characteristics. A complete discussion of the isotherm properties of rice husk adsorbents is still rare, while this is important for making it applicable and implementable for commercial and industries. Therefore, this study focused on investigating the adsorption properties of unmodified rice husk particles for removing dyes. Turmeric was selected as a model for organic dyes because it has an ideal molecular size (less than 1.4 nm) that is also suitable for evaluating and predicting the adsorbent-adsorbate interaction during the adsorption process. In contrast to previous studies, the novelty of this study was to evaluate the isotherm adsorption characteristics of rice husk particles in various particle sizes (i.e., 74, 177, and 500  $\mu\text{m}$ ). To confirm the phenomena during the adsorption process, we evaluated ten adsorption isotherms, including Langmuir, Freundlich, Temkin, Dubini-Radushkevich, Flory-Huggins, Fowler-Guggenheim, Hill DeBoer, Jovanovic, Harkin Jura, and Halsey. We focused on the particle size since the size itself has a direct impact on the availability of surface-active sites. In general, smaller particle size associates with the number of adsorption sites, giving ideas [9] for the possible modification in the adsorption process.

## 2. Literature Review

### 2.1 Agricultural Waste as Adsorbent

Seeing the economical and environmentally friendly adsorbents for water pollutant remediation and wastewater treatment, agricultural waste materials can be used as alternative resources for producing biosorbents. This is due to the high content of cellulose, hemicellulose, lignin, lipids, protein, starch, and other organic components, making it prospective to fulfill the requirements as a raw material for producing activated carbon [10]. Table 1 shows various agricultural wastes as adsorbents. Several raw materials were presented from the literature [11-30].

**Table 1**  
 Studies of dye adsorption using adsorbent from agricultural waste

Agricultural waste	Dyes	Ref.
<i>Chlorella Vulgaris</i>	Crystal violet	[11]
Corn cob	Methylene blue	[12]
Sugarcane bagasse	Methylene blue and crystal violet	[13]
Banana peel	Congo red	[14]
Watermelon rinds	Methylene blue dye	[15]
<i>Ziziphus jujube</i>	Methylene blue	[16]
Anchote peel	Indigo carmine	[17]
Rubber seed pericarp	Methyl orange	[18]
Citrus limetta peel	Methylene blue	[19]
Tea	Methylene blue and crystal violet d	[20]
Palm sugar fiber	Rhodamine-b	[21]
Sunflower seed hull	Methylene blue and methyl orange	[22]
Marigold flower	crystal violet	[23]
Sapindus seed	Basic yellow	[24]
Sesame seed	Yellow dye	[25]
Peanut husk	Methylene blue	[26]
Rice husk	Malachite green	[27]
Pineapple peel	Methylene blue and black b	[28]
Coconut waste	Methylene blue	[29]
Lemon leaf	Methylene blue	[30]

## 2.2 Adsorption Isotherm Theory

Adsorption is a surface phenomenon characterized by the attachment of atoms, ions, or molecules from a gas, liquid, or dissolved solid to the surface of a substance. A significant aspect of adsorption is the adsorption isotherm. Adsorption isotherm models are commonly used to obtain additional information about a process. Ten different isotherm models are used in this investigation: Langmuir, Freundlich, Temkin, Radosevich, Flory Huggins, Fowler-Guggenheim, Hill-DeBoer, Jovanovic, Harkin-Jura, and Halsey.

- i. **Langmuir.** This model defines the maximum adsorbent capacity as the presence of a single layer (monolayer) of adsorbate on the adsorbent surface. The rearranged Langmuir isotherm is represented by Eq. (1).

$$\frac{1}{Q_e} = \frac{1}{Q_{max} K_L C_e} + \frac{1}{Q_{max}} \quad (1)$$

where  $K_L$  is the Langmuir constant,  $q_e$  is the number of molecules adsorbed at equilibrium (mg/g), and  $q_m$  is the adsorption capacity (mg/g). In addition, the dimensionless constant, often known as the separation factor, is a crucial component of the Langmuir isotherm ( $R_L$ ) which is expressed by Eq. (2).

$$R_L = \frac{1}{1 + K_L C_e} \quad (2)$$

where  $R_L$  describes unfavorable adsorption ( $R_L > 1$ ); linear adsorption (affected by the amount and concentration of adsorbed molecules) ( $R_L = 1$ ); too strong adsorption or irreversible adsorption ( $R_L = 0$ ); and favorable adsorption or no desorption ( $0 < R_L < 1$ ).

- ii. **The Freundlich.** This model describes a type of physical adsorption in which the adsorption occurs in multiple layers, and the bonds are weak (multilayer). The Freundlich isotherm also explains the degree of linearity ( $n$ ) between the adsorbate solution and the adsorption process, which is described as follows:  $n = 1$ , linear adsorption;  $n < 1$ , adsorption process with chemical interaction;  $n > 1$ , adsorption process with physical interaction; Favorable adsorption process is declared when  $0 < \frac{1}{n} < 1$ , and a cooperative adsorption process occurs when  $\frac{1}{n} > 1$ .
- iii. **The Temkin.** This model evaluates the interaction between adsorbent and adsorbate, and the homogeneous distribution of binding energy over the surface of the adsorbent. The relation is given by Eq. (3).

$$Q_e = B_T \ln A_T + B_T \ln C_e \quad (3)$$

- iv. **The Dubinin-Radushkevich.** This model is used to obtain the average value of the adsorption-free energy ( $E$ ) as shown in Eq. (4).

$$E = \frac{1}{\sqrt{2\beta}} \quad (4)$$

- v. **The Jovanovic.** This model assumes no mechanical contact between the adsorbate and the adsorbent. The Jovanovic isotherm is shown by Eq. (5).

$$\ln Q_e = \ln Q_{max} - K_j C_e \quad (5)$$

- vi. **The Halsey.** This model evaluates a multilayer adsorption system. The calculation is shown in Eq. (6).

$$Q_e = \frac{1}{n_H} \ln K_H - \left(\frac{1}{n_H}\right) \ln C_e \quad (6)$$

- vii. **The Harkin jura.** This model explains the adsorption occurring on the adsorbent surfaces as multilayer adsorption due to the heterogeneous pore distribution of the adsorbent, as shown in Eq. (7).

$$\frac{1}{q_e^2} = \frac{\beta_{HJ}}{A_{HJ}} - \left(\frac{1}{A}\right) \log C_e \quad (7)$$

- viii. **The Flory-Huggins.** This model implies a spontaneous adsorption mechanism. The Flory-Huggins model is shown by Eq. (8).

$$\log \frac{\theta}{C_e} = \log K_{FH} + n \log(1 - \theta) \quad (8)$$

- ix. **The Fowler-Guggenheim.** This model described a Van der Waals contact effect between species adsorbed at adjacent locations. **The Fowler-Guggenheim** model is shown in Eq. (9).

$$\log \frac{\theta}{C_e} = \log K_{FH} + n \log(1 - \theta) \quad (9)$$

- x. **The Hill-DeBoer.** This model represents mobile adsorption and bilateral interactions between molecules that have been adsorbed. The Hill-DeBoer model is shown in Eq. (10).

$$\ln \left[ \frac{C_e(1-\theta)}{\theta} \right] - \frac{\theta}{1-\theta} = -\ln K_1 - \frac{K_2 \theta}{RT} \quad (10)$$

Equations of the used models are presented in Table 2. The prior study explains the detailed computation of isotherm adsorption [31,32].

**Table 2**

Isotherm models linear equations

Isotherm model	Linearized equation	Plotting
Langmuir	$\frac{1}{Q_e} = \frac{1}{Q_{max} K_L C_e} + \frac{1}{Q_{max}}$	$\frac{1}{C_e}$ vs $\frac{1}{Q_e}$
Freundlich	$\ln Q_e = \ln K_f + \frac{1}{n} \ln C_e$	$\ln C_e$ vs $\ln Q_e$
Temkin	$Q_e = B_T \ln A_T + B_T \ln C_e$	$\ln C_e$ vs $Q_e$
Dubinin-Radushkevich	$\ln Q_e = \ln Q_s - (\beta \varepsilon^2)$	$\varepsilon^2$ vs $\ln Q_e$
Halsey	$Q_e = \frac{1}{n_H} \ln K_H - \left(\frac{1}{n_H}\right) \ln C_e$	$\ln C_e$ vs $\ln Q_e$
Harkin-Jura	$\frac{1}{q_e^2} = \frac{\beta_{HJ}}{A_{HJ}} - \left(\frac{1}{A}\right) \log C_e$	$\log C_e$ vs $\frac{1}{q_e^2}$
Jovanovic	$\ln Q_e = \ln Q_{max} - K_j C_e$	$C_e$ vs $\ln Q_e$
Flory-Huggins	$\log \frac{\theta}{C_e} = \log K_{FH} + n \log(1 - \theta)$	$\log \left(\frac{\theta}{C_e}\right)$ vs $\log(1 - \theta)$
Fowler-Guggenheim	$\ln \left(\frac{C_e(1 - \theta)}{\theta}\right) - \frac{\theta}{1 - \theta} = -\ln K_{FG} - \frac{2W\theta}{RT}$	
Hill-DeBoer	$\ln \left[\frac{C_e(1 - \theta)}{\theta}\right] - \frac{\theta}{1 - \theta} = -\ln K_1 - \frac{K_2\theta}{RT}$	$\theta$ vs $\ln \left[\frac{C_e(1 - \theta)}{\theta}\right] - \frac{\theta}{1 - \theta}$

### 3. Methodology

#### 3.1 Preparation of the Adsorbent from Natural Rice Husk

The natural rice husk that was used in this study was acquired from a local market in Bandung, Indonesia. Before its use, the rice husk underwent saw-milling and was sifted through a sieve with varying hole sizes (500, 177, and 74  $\mu\text{m}$ ) which were obtained from Yayasan Bumi Publikasi Nusantara, Indonesia. This was done to determine its specific particle size.

#### 3.2 Characterization

To determine the morphological characterization of the material, a Scanning Electron Microscope (SEM; JSM-6360LA; JEOL Ltd., Japan) was used to characterize the Rice husk surface morphology and elemental analysis.

#### 3.3 Batch Adsorption Studies

In this study, turmeric was employed as a dye model to determine the adsorption characteristics of rice husk particles. Detailed information regarding the synthesis of turmeric solution can be seen in our previous research [33]. Adsorption experiments were carried out using a batch process. A glass batch reactor with a total volume of 200 mL contained a turmeric solution with various concentrations of 20, 40, 60, 80, and 100 ppm added to 0.05 g of rice husk (specific sizes 74, 177, and 500  $\mu\text{m}$ ). After that, the solution was shaken for one hour at 400 rpm at room temperature and a constant pH condition. The solution was then filtered using filter paper with a pore size of 0.22  $\mu\text{m}$ .

Blank solutions (turmeric solution without rice husk particle) at various concentrations were also tested under the same conditions and used as standard calibration. To examine changes in concentration, aliquots of solutions were examined using a Visible Spectroscope (Model 7205; JENWAY; Cole-Parmer; US) at maximum wavelengths in the range of 200 to 800 nm. The adsorption results were plotted and normalized. Then the maximum absorption peak was calculated using Beer's Law to obtain a constant concentration of turmeric.

## 4. Results and Discussion

### 4.1 Surface Characteristics of the Adsorbent

Figure 1 displays SEM analysis images of natural rice husks with varying particle sizes utilized in this research. As depicted in Figure 1, most particles exhibit low sphericity. However, a particle measuring 500  $\mu\text{m}$  in diameter possesses a nicely rounded shape, while a particle with a diameter of 177-74  $\mu\text{m}$  (see Figure 1 (b-c)) showcases a somewhat rounded form. Furthermore, smaller particles (Figure 1 (c)) exhibit a more uniform distribution.

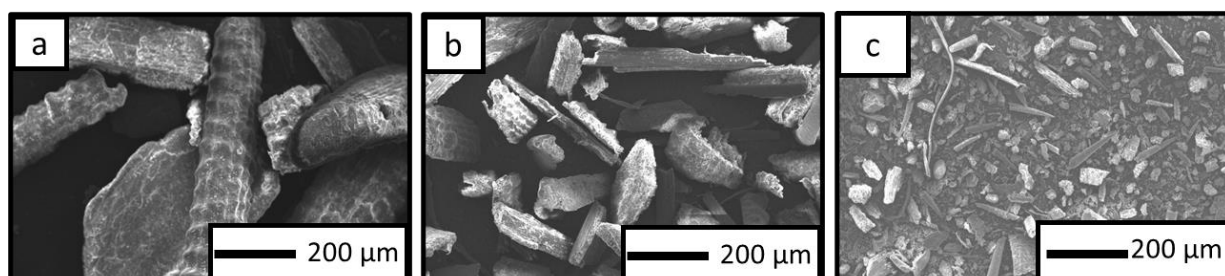


Fig. 1. SEM image of rice husk in different particle sizes: (a) 500 (b) 177 and (c) 74  $\mu\text{m}$

### 4.2 Adsorption Isotherm Studies

Adsorption isotherm analysis is essential for characterizing how the adsorbent surface interacts with adsorbate molecules and is widely used to get more details about the process. To find the most appropriate isotherm model, the experimental data were fitted with Langmuir, Freundlich, Temkin, Dubinin-Radushkevich, Flory Huggins, Fowler-Guggenheim, Hill-DeBoer, Jovanovic, Harkin-Jura, and Halsey. To investigate the model of adsorption, experimental data were analysed by a regression analysis to fit the linearized expression of mathematical models. The experimental values based on the plotting of some parameters are reconstituted (using plot equations in Table 2). Linear correlation coefficients ( $R^2 \geq 0.80$ ) are then used to show the compatibility of correlation curves between experimental data and linearized forms of the isotherm models. The plotting analysis can also derive several parameters in the adsorption process and predict what phenomena happening during the adsorption process. Table 3 presents the parameter obtained from the plotting analysis of isotherm models.

The Langmuir model states that a single layer of adsorbate covers the adsorbent surface without any interaction between the adsorbed molecules. The analysis of parameters indicated that the three particle sizes had a monolayer structure, with the smallest particle size having the highest adsorption capacity (687.40 mg/g). The  $K_L$  constant, also known as the Langmuir constant, is linked to the surface area and porosity of the adsorbent and indicates the degree of contact between the adsorbate and the surface, reflecting the sorption energy [31]. A high  $K_L$  value suggests a strong bond between the adsorbate and adsorbent, while a low value indicates a weak connection. The obtained  $K_L$  value suggests a weak connection between the adsorbent and adsorbate, indicating that the adsorption

process may form a multilayer structure (even though the correlation coefficient values are great ( $R^2 > 0.80$ )) where adsorbate molecules are not distributed evenly on all adsorbent surfaces. The  $R_L$  analysis showed that rice husk particles have properties under favourable conditions ( $0 < R_L < 1$ ) where the adsorption process can be controlled by changing process variables [32].

The Freundlich model is often utilized to clarify adsorption in systems that are not uniform. The analysis of the graphs indicates that the  $R^2$  values for particles of all sizes are outstanding ( $R^2 > 0.80$ ), demonstrating that adsorption transpires on a varied surface in multiple layers with minimal interaction between the adsorbate and adsorbent. The assessment of the  $n$  value for rice husk particles revealed that the correlations of  $n$  were less than zero and  $1/n$  was greater than zero for particles of all sizes, indicating a favourable chemical interaction.

The Temkin model, as shown in Table 3, demonstrates that the adsorbate on the surface area of the adsorbent is not evenly spread out. This is evident from the  $R^2$  values of all particle sizes, which were above 0.80. The  $B_T$  result reveals that values below 8 kJ/mol suggest that the particles experienced physical interaction. Furthermore, the negative  $B$  and  $B_T$  values indicate that the adsorption process is endothermic.

In this study, the Dubinin-Radushkevich model exhibited the lowest  $R^2$  value. When the particle sizes were 500 and 177  $\mu\text{m}$ , there was pore-filling present on the adsorbent surface, but no pore-filling was formed when the size was 74  $\mu\text{m}$ . The results suggest that the adsorption process did not follow this model based on the  $R^2$  value. Additionally, evaluating the  $E$  value in this model suggests that the adsorption process occurs physically ( $E < 8$  kJ/mol).

The Flory Huggins isotherm model assumes that polymer segments occupy lattice sites and solvent molecules occupy single sites. This model explains how the adsorption process occurs and determines if it is possible and spontaneous. The Flory-Huggins isotherm shows that multiple layers of adsorbate molecules are formed on the biosorbent surface for all particle sizes. Although the correlation coefficient is high ( $R^2 > 0.80$ ), the  $n_{FH}$  result is negative, indicating that more than one active adsorbent zone is occupied by the adsorbate. By using the  $K_{FH}$  equilibrium constant derived from the Flory-Huggins isotherm equation, the Gibbs free energy ( $\Delta G^\circ$ ) of spontaneity can be determined. The  $\Delta G$  values for turmeric adsorption were negative for all particle sizes, indicating that the adsorption process is spontaneous [31,32].

The analysis conducted by Fowler Guggenheim on the  $R^2$  values indicates that all particle sizes have excellent values ( $R^2 > 0.80$ ), suggesting multilayer adsorption. The analysis of  $W$  values revealed that the adsorbed molecules repel each other ( $W = \text{negative}$ ), leading to an endothermic process. This causes some of the molecules to not bind due to weak interactions caused by Van der Waals forces (physical interactions). Additionally, the repulsive interactions also result in a decrease in the heat of adsorption as the load increases. This finding aligns with the Temkin model.

The Hill-de Boer analysis shows an excellent correlation coefficient value ( $R^2 > 0.80$ ) indicating the involvement of multilayer structure in the adsorption process. The values of  $K_2$  confirmed that there is repulsion between the adsorbed molecules, which is in good agreement with The Temkin and Fowler Guggenheim models.

The Jovanovic isotherm showed excellent adsorption capacity, yielding 1072.98; 1205.88; and 1067 mg/g for particle sizes of 500, 177, and 74  $\mu\text{m}$  respectively. In addition, the  $R^2$  values obtained from this model were also very high ( $R^2 > 0.80$ ) indicating a monolayer structure.

The Harkins-Jura isotherm is explained by the presence of a heterogeneous pore distribution, which leads to multilayer adsorption. The high correlation coefficient value of adsorption using rice husk makes it a suitable method. The small value of  $B_{HJ}$  in the Harkin Jura parameter is linked to the specific surface area [31]. The correlation coefficient values ( $R^2$ ) indicate a multilayer structure for all particle sizes.

The Halsey model is appropriate for assessing the adsorption of adsorbate ions in a multilayer adsorption system, particularly when the adsorption occurs at a considerable distance from the surface [31]. Like the Freundlich isotherm model, the Halsey model is also suitable for multilayer adsorption and heterogeneous surfaces where the distribution of adsorption heat is not uniform [33]. The significant result is indicated by the correlation coefficient ( $R^2$ ) value of this model indicating multilayer adsorption.

**Table 3**

The parameter value of the isotherm model of turmeric dye on rice husk in various size particles

Isotherm models	Parameter	Particle size			Note
		500	177	74	
Langmuir	$Q_{max}$ (mg/g)	681.40	361.48	687.40	Adsorption capacity maximum(mg/g)
	$K_L$ (L/mg)	-0.138	-0.04	-0.213	The Langmuir model constant
	$R_L$	0.244	1.5784	0.488	Favourable adsorption process ( $0 < R_L < 1$ )
	$R^2$	0.934	0.831	0.842	$R^2 < 0.80$ , multilayer formation on the adsorbent surface $R^2 > 0.80$ , monolayer formation on the adsorbent surface
Freundlich	$K_f$ (mg/g)	0.788	0.537	0.811	The Freundlich model constant
	$1/n$	0.24	0.62	0.21	Favourable adsorption ( $0 < 1/n < 1$ )
	$n_f$	-4.20	-1.61	-4.79	Chemical adsorption process ( $n < 1$ )
	$R^2$	0.984	0.952	0.960	$R^2 > 0.80$ , multilayer formation on the adsorbent surface $R^2 < 0.80$ , monolayer formation on the adsorbent surface
Temkin	$AT$ (L/g)	0	0	0	The binding constant for the Temkin equilibrium
	$B$	-199.54	-378.20	-10382	The Temkin constant
	$BT$ (KJ/mol)	0.123	-0.065	-0.141	Physical process adsorption ( $\beta_T < 8$ kJ/mol)
	$R^2$	0.989	0.984	0.972	$R^2 < 0.80$ , homogenous adsorbent surface $R^2 > 0.80$ , heterogeneous adsorbent surface
Dubinin-Radushkevich	$\beta$ (mol <sup>2</sup> /kJ <sup>2</sup> )	0.276	2.126	0.112	The Dubinin-Radushkevich model constant
	$E$ (kJ/mol)	1.345	0.485	2.107	Physical process adsorption ( $E < 8$ kJ/mol)
	$R^2$	0.892	0.837	0.749	$R^2 > 0.80$ , micropore size exists in adsorbent surface $R^2 < 0.80$ , no micropore size exists in adsorbent surface
Flory Huggins	$n_{FH}$	-4.131	-1.534	-4.601	$n_{FH} < 1$ , represents the multi-active adsorbent zone occupied by the adsorbate
	$K_{FH}$ (L/mg)	$1.99 \times 10^{-11}$	$4.26 \times 10^{-5}$	$1.21 \times 10^{-12}$	Flory–Huggins model constant
	$\Delta G^\circ$ (kJ/mol)	-604.486	-246.866	-673.066	$\Delta G < 0$ , informing spontaneous process
	$R^2$	0.984	0.953	0.960	$R^2 > 0.80$ , multilayer formation on the adsorbent surface

					$R^2 < 0.80$ , monolayer formation on the adsorbent surface
Fowler Guggenheim	$W$ (kJ/mol)	-11.62	-7.18	-12.91	$W < 0$ , repulsive interaction between adsorbed species
	$KFG$	$9.26 \times 10^{-6}$	0.000283	$4.39 \times 10^{-6}$	The Fowler Guggenheim model constant
	$R^2$	0.992	0.995	0.978	$R^2 > 0.80$ , multilayer formation on the adsorbent surface $R^2 < 0.80$ , monolayer formation on the adsorbent surface
Hill-de Boer	$K_1$ (L/mg)	$1.48 \times 10^{-13}$	$1.72 \times 10^{-5}$	$2.2 \times 10^{-17}$	The Hill-Deboer model constant
	$K_2$ (kJ/mol)	-1187.1	-468.053	-1401	Repulsive interaction between adsorbed species
	$R^2$	0.969	0.974	0.913	$R^2 > 0.80$ , multilayer formation on the adsorbent surface $R^2 < 0.80$ , monolayer formation on the adsorbent surface
Jovanovic	$KJ$	-0.006	-0.008	-0.006	The Jovanovic model constant
	$Q_{max}$ (mg/g)	1072.99	1205.88	1067.03	Adsorption capacity maximum (mg/g)
	$R^2$	0.999	0.991	0.999	$R^2 < 0.80$ , multilayer formation on the adsorbent surface $R^2 > 0.80$ , monolayer formation on the adsorbent surface
Harkin Jura	$AH_j$	637	115	713	The Harkin Jura model constant
	$B_H$ (L/mg)	0.691	1.502	0.475	The specific surface area of the adsorbent
	$R^2$	0.970	0.841	0.930	$R^2 > 0.80$ , multilayer formation on the adsorbent surface $R^2 < 0.80$ , monolayer formation on the adsorbent surface
Halsey	$n_H$	-4.200	-1.610	-4.792	Halsey model constant
	$K_H$ (L/mg)	2019	8832	1744	Halsey model constants.
	$R^2$	0.984	0.953	0.960	$R^2 > 0.80$ , multilayer formation on the adsorbent surface $R^2 < 0.80$ , monolayer formation on the adsorbent surface

Furthermore, based on the  $R^2$  fitting value analysis, the adsorption of turmeric with rice husk particles of varying sizes demonstrates different levels of compatibility. Specifically, for the largest particle size (500  $\mu\text{m}$ ), the most suitable adsorption model is Jovanovic, followed by Fowler Guggenheim, Temkin, Freundlich, Flory Huggins, Halsey, Harkin Jura, Hill-de Boer, Langmuir, and Dubinin-Radushkevich. For medium-sized particles (177  $\mu\text{m}$ ), the order of suitability is Fowler Guggenheim, Jovanovic, Temkin, Hill-de Boer, Freundlich, Flory Huggins, Halsey, Dubinin-Radushkevich, and Langmuir. For the finest particle size used in this study (74  $\mu\text{m}$ ), the most suitable isotherm models are Jovanovic, Fowler Guggenheim, Temkin, Freundlich, Halsey, Flory Huggins, Harkin Jura, Hill-de Boer, Langmuir, and Dubinin-Radushkevich.

According to the findings presented in Table 3, all isotherm models agree with the experimental data. The negative value of the Gibbs free energy for all models indicates that the adsorption process occurs spontaneously. The  $R^2$  analysis shows that the Jovanovic model applies to all particles size (the highest  $R^2$  value), suggesting that the adsorption process takes place in a monolayer [31]. The adsorption of adsorbate molecules onto the surface of the adsorbent is a physically favourable

interaction, which can be controlled by adjusting the process conditions [32]. The Langmuir model confirms the monolayer model, indicating that molecules are distributed uniformly across the adsorbent surface. The  $RL$  values, ranging between 0 and 1, indicate a normal and favourable adsorption process that can be controlled by modifying the process conditions. The Fowler-Guggenheim model supported the idea that molecules in a multilayer structure repel each other (repulsive interaction). This model had the second-highest value for  $R^2$ . The Temkin model showed that adsorption is a physical process and that the adsorbent surface is heterogeneous, which corresponds with the  $R^2$  value in Jovanovic and Langmuir. The Dubinin-Radushkevich model also confirmed physical adsorption, with the presence of micropores on the adsorbent surface. The Freundlich model indicated chemical adsorption, which is favourable. The Flory-Huggins model suggested that there are multiple active adsorbent zones occupied by the adsorbate. The Hill-de Boer model supported the Fowler-Guggenheim model's idea of repulsive interaction between adsorbed species. The Halsey and Harkin Jura models confirmed multilayer adsorption. Even though the models align with experimental results, the adsorption profile follows physical adsorption (although chemisorption may be formed during the adsorption process) with multilayer adsorption. From the results of the experimental analysis in Table 3, it can be concluded that the adsorption mechanism is presented in Figures 2 (a) and (b). When a small adsorbent (74  $\mu\text{m}$ ) is used, the adsorption system forms a multilayer surface without pore filling, which occurs endothermically with repulsive intermolecular interactions (see Figure 2(a)). However, a different mechanism was found when large (500  $\mu\text{m}$ ) and medium (177  $\mu\text{m}$ ) adsorbents were used. The adsorption process occurred endothermically by forming a multilayer surface with a pore-filling system and repulsive intermolecular interactions (see Figure 2 (b)).

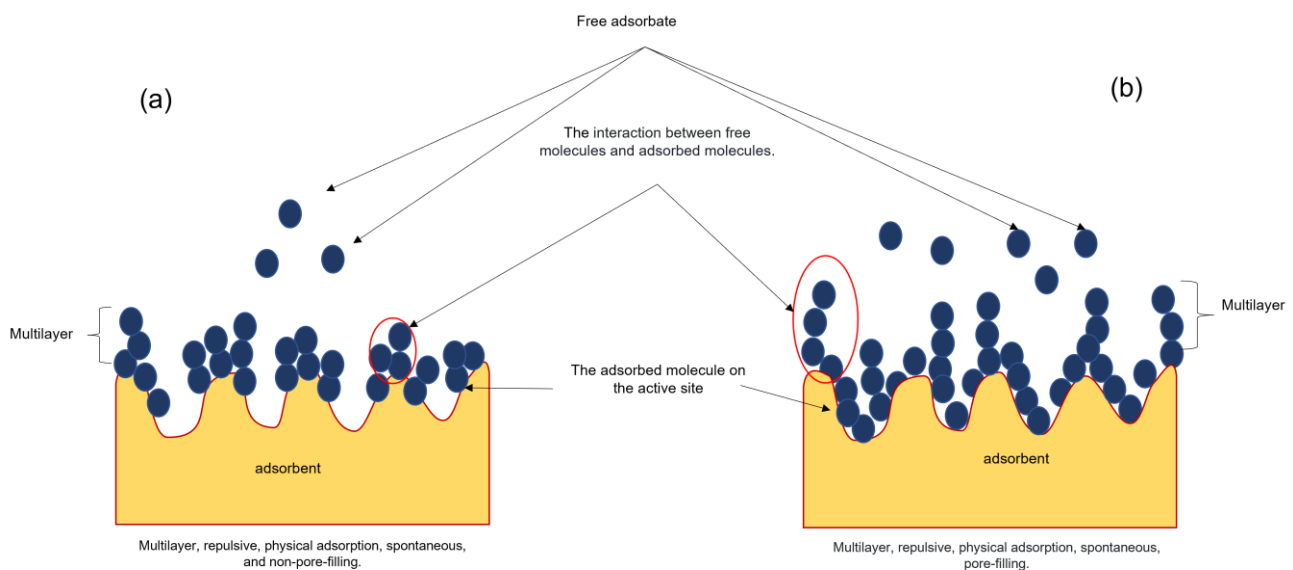


**Fig. 2.** The proposed illustration of the adsorption mechanism of rice husk with various particle sizes: (a) particle size 74  $\mu\text{m}$  and (b) particle sizes 500 and 177  $\mu\text{m}$

## 5. Conclusion

The present study investigates the adsorption properties of natural rice husks of different sizes (specifically, 74, 177, and 500  $\mu\text{m}$ ) as a means of adsorbing dye. Ten models were used to analyze the adsorption isotherms, including Langmuir, Freundlich, Temkin, Dubinin-Radushkevich, Flory Huggins, Fowler-Guggenheim, Hill DeBoer, Jovanovic, Harkin Jura, and Halsey, by examining the correlation

coefficient values. The adsorption process occurs through the formation of a multilayer with physical interaction and repulsion between the adsorbent and adsorbate for all particles size. The results also stated that for large (500  $\mu\text{m}$ ) and medium (177  $\mu\text{m}$ ) adsorbents, pore filling occurred. Meanwhile, the small adsorbent (74  $\mu\text{m}$ ) did not fill the pores. This study offers insights into the adsorption phenomena associated with the use of natural rice husk for removing Turmeric dye from an aqueous solution.

## Acknowledgment

This research was funded by BRIN and Universitas Pendidikan Indonesia (Grant: Bangdos).

## References

- [1] Permatasari, Novie, Transmissia Noviska Suchaya, and Asep Bayu Dani Nandiyanto. "Agricultural wastes as a source of silica material." *Indonesian Journal of Science and Technology* 1, no. 1 (2016): 82-106. <https://doi.org/10.17509/ijost.v1i1.8619>
- [2] Pramesti, K. A., R. A. Kusumadewi, and R. Hadisoebroto. "The effect of mixing speed and contact time on the process of dye adsorption using corncobs adsorbent." *IOP Conference Series: Earth and Environmental Science*, 737, no. 1 (2021): 012014. <https://doi.org/10.1088/1755-1315/737/1/012014>
- [3] Nandiyanto, A. B. D., A. S. Wiryani, A. Rusli, A. Purnamasari, A. G. Abdullah, I. Widiaty, and R. Hurriyati. "Extraction of curcumin pigment from Indonesian local turmeric with its infrared spectra and thermal decomposition properties." *IOP Conference Series: Materials Science and Engineering*, 180, no. 1 (2017): 012136. <https://doi.org/10.1088/1757-899X/180/1/012136>
- [4] Anshar, Andi Muhammad, Paulina Taba, and Indah Raya. "Kinetic and thermodynamics studies the adsorption of phenol on activated carbon from rice husk activated by  $\text{ZnCl}_2$ ." *Indonesian Journal of Science and Technology* 1, no. 1 (2016): 47-60. <https://doi.org/10.17509/ijost.v1i1.2213>
- [5] Bintoro, Nursigit, and Alya Iqlima Zahra. "Effects of Moisture Content and Grain Type on Mechanical Properties of White Rice: Literature review and Experiment." *Indonesian Journal of Science and Technology* 7, no. 2: 337-362. <https://doi.org/10.17509/ijost.v7i2.50887>
- [6] Wulandari, Aulia Eka, Sekar Madu Kusumawardani, Mutiara Amelia Sabrina, Sofi Arofah, Siti Nur Shifa Sholihat, Dadi Rusdiana, Tri Suwandi, and Muhammad Aziz. "Design of rice husks gasification stove." *ASEAN Journal of Science and Engineering* 1, no. 1 (2021): 1-8. <https://doi.org/10.17509/ajse.v1i1.33644>
- [7] Nurjamil, A. M., N. A. Wolio, R. N. Laila, S. A. Rohmah, Asep Bayu Dani Nandiyanto, Sri Anggraeni, and Tedi Kurniawan. "Eco-friendly batteries from rice husks and wood grain." *ASEAN Journal of Science and Engineering* 1, no. 1 (2021): 45-48. <https://doi.org/10.17509/ajse.v1i1.33768>
- [8] Nandiyanto, Asep Bayu Dani, Siti Nur Hofifah, Hilma Tahsilul Inayah, Silmi Ridwan Putri, Siti Saffanah Apriliani, Sri Anggraeni, Dian Usdiyana, and Ali Rahmat. "Adsorption isotherm of carbon microparticles prepared from pumpkin (*Cucurbita maxima*) seeds for dye removal." *Iraqi Journal of Science* (2021): 1404-1414. <https://doi.org/10.24996/ijs.2021.62.5.2>
- [9] Nurjamil, Aris Muhamad, Nurmiyati Annisa Wolio, Rahma Nur Laila, Silmi Aulia Rohmah, Sri Anggraeni, and Asep Bayu Dani Nandiyanto. "Effect of Rice Husks and Wood Grain as Electrolyte Adsorbers on Battery." *Indonesian Journal of Multidisciplinary Research* 1, no. 1: 69-72. <https://doi.org/10.17509/ijomr.v1i1.33778>
- [10] Pathak, Pranav D., Sachin A. Mandavane, and Bhaskar D. Kulkarni. "Fruit peel waste as a novel low-cost bio adsorbent." *Reviews in Chemical Engineering* 31, no. 4 (2015): 361-381. <https://doi.org/10.1515/revce-2014-0041>
- [11] Kiew, Peck Loo, Nur Ainaa Mohd Fauzi, Shania Afaa Firdiani, Man Kee Lam, Lian See Tan, and Wei Ming Yeoh. "Iron oxide nanoparticles derived from *Chlorella vulgaris* extract: Characterization and crystal violet photodegradation studies." *Progress in Energy and Environment* (2023): 1-10.
- [12] Medhat, Ahmed, Heba H. El-Maghrabi, Amr Abdelghany, Nabil M. Abdel Menem, Patrice Raynaud, Yasser M. Moustafa, Mohamed A. Elsayed, and Amr A. Nada. "Efficiently activated carbons from corn cob for methylene blue adsorption." *Applied Surface Science Advances* 3 (2021): 100037. <https://doi.org/10.1016/j.apsadv.2020.100037>
- [13] Alnasrawy, Shaimaa Taleb. "Adsorption Efficiency, Isotherms, and Kinetics for Cationic Dye Removal Using Biowaste Adsorbent." *Journal of Hazardous, Toxic, and Radioactive Waste* 27, no. 1 (2023): 04022040. [https://doi.org/10.1061/\(ASCE\)HZ.2153-5515.0000735](https://doi.org/10.1061/(ASCE)HZ.2153-5515.0000735)
- [14] Mondal, Naba Kumar, and Sumana Kar. "Potentiality of banana peel for removal of Congo red dye from aqueous solution: isotherm, kinetics and thermodynamics studies." *Applied Water Science* 8 (2018): 1-12. <https://doi.org/10.1007/s13201-018-0811-x>

- [15] Shukla, Saurabh, Ramsha Khan, Mahendra Mohan Srivastava, and Sasan Zahmatkesh. "Valorization of Waste Watermelon Rinds as a Bio-adsorbent for Efficient Removal of Methylene Blue Dye from Aqueous Solutions." *Applied Biochemistry and Biotechnology* (2023): 1-15. <https://doi.org/10.1007/s12010-023-04448-3>
- [16] Satouh, Sara, Salim Bousba, Nabil Bougdah, Charf Eddine Bounoukta, Sabrina Halladja, and Nabil Messikh. "A Ziziphus jujuba waste-derived biochar as a low-cost adsorbent for the removal of Indigo carmine dye from aqueous solution." *DESALINATION AND WATER TREATMENT* 289 (2023): 258-270. <https://doi.org/10.5004/dwt.2023.29445>
- [17] Hambisa, Agesa Abdisa, Melkamu Biyana Regasa, Haile Gurmessa Ejigu, and Chala Boru Senbeto. "Adsorption studies of methyl orange dye removal from aqueous solution using Anchote peel-based agricultural waste adsorbent." *Applied Water Science* 13, no. 1 (2023): 24. <https://doi.org/10.1007/s13201-022-01832-y>
- [18] Jawad, Ali H., Nurul Najwa Abd Malek, Tumirah Khadiran, Zeid A. AlOthman, and Zaher Mundher Yaseen. "Mesoporous high-surface-area activated carbon from biomass waste via microwave-assisted-H3PO4 activation for methylene blue dye adsorption: An optimized process." *Diamond and Related Materials* 128 (2022): 109288. <https://doi.org/10.1016/j.diamond.2022.109288>
- [19] Rani, Sonia, and Sudesh Chaudhary. "Adsorption of methylene blue and crystal violet dye from waste water using Citrus limetta peel as an adsorbent." *Materials Today: Proceedings* 60 (2022): 336-344. <https://doi.org/10.1016/j.matpr.2022.01.237>
- [20] Wulandari, Meyliana, Nofrizal Nofrizal, and Syed Azhar Syed Sulaiman. "Tea waste products: A new low-cost and green adsorbent alternative for rhodamine-B dye removal." *Indonesian Journal of Chemistry* (2022). <https://doi.org/10.22146/ijc.75739>
- [21] Mahardiani, Lina, Pundung Setia Lesana, and Sulisty Saputro. "Chemical approach for the synthesis of nanofibers from sugar palm fiber as a functional adsorbent modified with cobalt oxide to remove dye waste." *Key Engineering Materials* 920 (2022): 95-105. <https://doi.org/10.4028/p-sg82a6>
- [22] Anastopoulos, Ioannis, Georgios Giannopoulos, Azharul Islam, Joshua O. Ighalo, Felicitas U. Iwuchukwu, Ioannis Pashalidis, Dimitrios Kalderis, Dimitrios A. Giannakoudakis, Vaishakh Nair, and Eder C. Lima. "Potential environmental applications of Helianthus annuus (sunflower) residue-based adsorbents for dye removal in (waste) waters." *Biomass-Derived Materials for Environmental Applications*, pp. 307-318. Elsevier, 2022. <https://doi.org/10.1016/B978-0-323-91914-2.00008-8>
- [23] Verma, Lata, Dipti Sonkar, Chandra Bhan, Jiwan Singh, Utkarsh Kumar, B. C. Yadav, and Ashish Nayak. "Adsorptive performance of Tagetes flower waste based adsorbent for crystal violet dye removal from an aqueous solution." *Environmental Sustainability* 5, no. 4 (2022): 493-506. <https://doi.org/10.1007/s42398-022-00250-9>
- [24] Sidiqua, M. Ayisha, and V. S. Priya. "Removal of yellow dye using composite binded adsorbent developed using natural clay and activated carbon from sapindus seed." *Biocatalysis and Agricultural Biotechnology* 33 (2021): 101965. <https://doi.org/10.1016/j.bcab.2021.101965>
- [25] Yilmaz, Pelin, Davut Gunduz, and Belma Ozbek. "Utilization of low-cost bio-waste adsorbent for methylene blue dye removal from aqueous solutions and optimization of process variables by response surface methodology approach." *Desal Water Treat* 224 (2021): 367-388. <https://doi.org/10.5004/dwt.2021.27206>
- [26] Ali, Asmadi, Alex Wong Chung Ing, Wan Rafizah Wan Abdullah, Sofiah Hamzah, and Fazureen Azaman. "Preparation of high-performance adsorbent from low-cost agricultural waste (Peanut husk) using full factorial design: Application to dye removal." *Biointerface Research Applied Chemistry* 10 (2020): 6619-6628. <https://doi.org/10.33263/BRIAC106.66196628>
- [27] Abd-elnaeem, Sara G., Azza I. Hafez, Rania M. Sabry, and T. E. Shakinis. "Removal of dyes by using rice husk as agricultural solid waste adsorbent: Experimental investigation." *Challenging Issues on Environment and Earth Science* 7 (2021): 64-79. <https://doi.org/10.9734/bpi/ciees/v7/10606D>
- [28] Krishni, R. R., K. Y. Foo, and B. H. Hameed. "Food cannery effluent, pineapple peel as an effective low-cost biosorbent for removing cationic dye from aqueous solutions." *Desalination and Water Treatment* 52, no. 31-33 (2014): 6096-6103. <https://doi.org/10.1080/19443994.2013.815686>
- [29] Kocaman, Suheyla. "Synthesis and cationic dye biosorption properties of a novel low-cost adsorbent: coconut waste modified with acrylic and polyacrylic acids." *International Journal of Phytoremediation* 22, no. 5 (2020): 551-566. <https://doi.org/10.1080/15226514.2020.1741509>
- [30] Sarath Babu, B., and G. Yamini. "Removal of methylene blue dye by using lemon leaf powder as an adsorbent." *Recent trends in waste water treatment and water resource management* (2020): 101-109. [https://doi.org/10.1007/978-981-15-0706-9\\_10](https://doi.org/10.1007/978-981-15-0706-9_10)
- [31] Ragadhita, Risti, and Asep Bayu Dani Nandiyanto. "How to calculate adsorption isotherms of particles using two-parameter monolayer adsorption models and equations." *Indonesian Journal of Science and Technology* 6, no. 1 (2021): 205-234. <https://doi.org/10.17509/ijost.v6i1.32354>
- [32] Nandiyanto, Asep Bayu Dani, Rina Maryanti, Meli Fiandini, Risti Ragadhita, Dian Usdiyana, Sri Anggraeni, Wafa Raihana Arwa, and Abdulkareem Sh Mahdi Al-Obaidi. "Synthesis of carbon microparticles from red dragon fruit

- (Hylocereus undatus) peel waste and their adsorption isotherm characteristics." *Molekul* 15, no. 3 (2020): 199-209. <https://doi.org/10.20884/1.jm.2020.15.3.657>
- [33] Nandiyanto, A. B. D., A. S. Wiryani, A. Rusli, A. Purnamasari, A. G. Abdullah, I. Widiaty, and R. Hurriyati. "Extraction of curcumin pigment from Indonesian local turmeric with its infrared spectra and thermal decomposition properties." *IOP Conference Series: Materials Science and Engineering* 180, no. 1 (2017), 012136. <https://10.1088/1757-899X/180/1/012136>